OXFORD UNIVERSITY PRESS | Schizophrenia Bulletin

Altered temporal dynamics of resting-state fMRI in adolescent-onset first-episode psychosis

Journal:	*Schizophrenia Bulletin*
Manuscript ID	SZBLTN-ART-22-0612.R2
Manuscript Type:	Regular Article
Date Submitted by the Author:	28-May-2023
Complete List of Authors:	Masias Bruns, Mireia; Universitat Pompeu Fabra, Department of Information and Communications Technologies Ramirez-Mahaluf, Juan ; Pontificia Universidad Católica de Chile, Psychiatry Valli, Isabel; August Pi i Sunyer Institute of Biomedical Research, ; Institute of Psychiatry Psychology and Neuroscience, Psychosis Studies Ortuño, Maria; Institut d'Investigacions Biomediques August Pi i Sunyer Ilzarbe, Daniel; Hospital Clinic de Barcelona, Child and Adolescent Psychiatry and Psychology; August Pi i Sunyer Institute of Biomedical Research, de la Serna, Elena; Department of Child and Adolescent Psychiatry and Psychology, Institute of Neurosciences, Hospital Clinic of Barcelona, Spain; Centro de Investigación Biomédica en Red de Salud Mental (CIBERSAM), Spain, Puig, Olga; Hospital Clinic de Barcelona, Child and Adolescent Psychiatry and Psychology, 2017SGR881; CIBERSAM, Centro Investigación Biomédica en Red Salud Mental Crossley, Nicolas; Pontificia Universidad Católica de Chile, González Ballester, Miguel Ángel; Universitat Pompeu Fabra, Department of Information and Communications Technologies; Instituciò Catalana de Recerca i Estudis Avancats Baeza, Emmaculata; Hospital Clinic de Barcelona, Child and adolescent Psuchiatry and Psychology department Piella, Gemma; Universitat Pompeu Fabra, Department of Information and Communications Technologies Castro, Josefina; Hospital Clínic of Barcelona. Insitute of Neurociences, Deparatment of Child and Adolescent Psychiatry and Psychology Sugranyes, Gisela; Hospital Clinic Barcelona, Child and Adolescent Psychiatry and Psychology
Keywords:	Adolescent Onset-Psychosis, resting-state fMRI, Temporal Connectivity Patterns, Graph Analysis, dynamic Functional Connectivity

Altered temporal dynamics of resting-state fMRI in adolescent-onset first-episode psychosis

Mireia Masias[a] (MSc; mireia.masias@upf.edu), Juan Pablo Ramirez-Mahaluf[b,1] (MD, PhD; jpramirezmahaluf@gmail.com), Isabel Valli*[c] (MD, PhD; valli@clinic.cat), María Ortuño[c] (MSc; mmortuno@recerca.clinic.cat), Daniel Ilzarbe[c,d,e,f] (MD, PhD; dilzarbe@clinic.cat), Elena De la Serna[d,e,2] (PhD; eserna@clinic.cat), Olga Puig-Navarro[d,e] (PhD, opuig@clinic.cat), Nicolas Crossley[b] (MD, PhD; ncrossley@uc.cl), Miguel Angel González Ballester[a,g,3] (PhD; ma.gonzalez@upf.edu), Inmaculada Baeza[c,d,e,f] (MD, PhD; ibaeza@clinic.cat), Gemma Piella[a] (PhD; gemma.piella@upf.edu), Josefina Castro-Fornieles[c,d,e,f] (MD, PhD; jcastro@clinic.cat), Gisela Sugranyes[c,d,e,f,*] (MD, PhD; gernest@clinic.cat)

[a]*BCN-MedTech, Universitat Pompeu Fabra, Barcelona, Spain.*

[b]*Department of Psychiatry, School of Medicine, Pontificia Universidad Católica de Chile, Santiago, Chile.*

[c]*Institut d'Investigacions Biomèdiques Agustí Pi i Sunyer (IDIBAPS), Barcelona, Spain.*

[d]*Department of Child and Adolescent Psychiatry, 2017SGR881, Institute of Neuroscience, Hospital Clínic de Barcelona, Barcelona, Spain.*

[e]*Centro de Investigación Biomédica en Red de Salud Mental (CIBERSAM), Instituto de Salud Carlos III, Spain.*

[f]*Department of Medicine, Universitat de Barcelona, Barcelona, Spain.*

[g]*ICREA, Barcelona, Spain.*

* Corresponding authors.

Isabel Valli (MD, PhD)

Institut d'Investigacions Biomèdiques August Pi i Sunyer (IDIBAPS). C/Rosselló, 149, 08036, Barcelona (Spain)

Email: valli@clinic.cat

Gisela Sugranyes (MD, PhD)

Institut d'Investigacions Biomèdiques August Pi i Sunyer (IDIBAPS). Department of Child and Adolescent Psychiatry and Psychology, Institute of Neuroscience,Hospital Clinic de Barcelona. C/ Villarroel 170, 08036 Barcelona (Spain).

Telephone: (34) 93 2279974. Fax: (34) 93 2279172. Email: *gernest@clinic.cat*

Word count

Abstract: 249 words.

Text body: 3995 words.

Abstract

Background. Dynamic functional connectivity (dFC) alterations have been reported in patients with adult-onset and chronic psychosis. We sought to examine whether such abnormalities were also observed in patients with first episode, adolescent-onset psychosis (AOP), in order to rule out potential effects of chronicity and protracted antipsychotic treatment exposure. AOP has been suggested to have less diagnostic specificity compared to psychosis with onset in adulthood and occurs during a period of neurodevelopmental changes in brain functional connections.

Study Design. Seventy-nine patients with first episode, AOP (36 patients with Schizophrenia Spectrum Disorder, SSD; and 43 with Affective psychotic disorder, AF) and 54 healthy controls (HC), aged 10 to 17 years were included. Participants underwent clinical and cognitive assessments and resting-state functional magnetic resonance imaging. Graph-based measures were used to analyze temporal trajectories of dFC, which were compared between patients with SSD, AF, and HC. Within patients, we also tested associations between dFC parameters and clinical variables.

Study Results. Patients with SSD temporally visited the different connectivity states in a less efficient way (reduced global efficiency), visiting fewer nodes (larger temporal modularity, and increased immobility), with a reduction in the metabolic expenditure (cost and leap size), relative to AF and HC (effect sizes: Cohen's D, ranging 0.54 to .91). In youth with AF, these parameters did not differ compared to HC. Connectivity measures were not associated with clinical severity, intelligence, cannabis use or dose of antipsychotic medication.

Conclusion. dFC measures hold potential towards the development of brain-based biomarkers characterizing adolescent-onset SSD.

Keywords: Adolescent Onset-Psychosis, resting-state fMRI, Temporal Connectivity Patterns, Graph Analysis, dynamic Functional Connectivity.

1. Introduction

First episode psychosis often presents with a combination of psychotic and affective symptoms and longitudinal assessments may be necessary to establish diagnosis. This holds treatment and prognostic implications and is especially relevant in adolescent-onset psychosis (AOP) since onset of psychosis during adolescence has been associated with a lower level of diagnostic specificity of clinical presentations than when it occurs in adulthood[1,2]. However, there is still a lack of objective, brain-based biomarkers with diagnostic and prognostic potential in psychiatry.

The *Disconnection Hypothesis*[3] suggests that the primary pathophysiological mechanism underlying psychosis is synaptic in nature. Functional connectivity abnormalities measured using resting-state functional magnetic resonance imaging (rs-fMRI), which quantifies the blood oxygen level dependent (BOLD) signal of the brain in the absence of a task, have been observed both in schizophrenia-spectrum disorders (SDD) and affective psychoses (AF, bipolar and depressive disorders with psychotic symptoms), including a diffuse alteration of brain connectivity[5–8] and a reduction in the number of hubs or regions with a significant contribution to brain functional networks[9,10]. However, the reported alterations are not consistent across all studies[11] and they do not permit to disentangle whether the observed rsfMRI changes are caused by synaptic abnormalities or structural constraints. Methods capable of profiling rs-fMRI dynamics, known as dynamic functional connectomics (dFC), have the potential to better describe the non-stationary[12] nature of brain connectomics, which are likely to be especially prominent when mental activity is unconstrained[13]. Additionally, dFC methods are considered less dependent on structural connections and more capable to identify changes specifically related with neural population dynamics[14].

Most dFC studies to date focused on the spatial organization of different temporal connectivity patterns, activated during the rs-fMRI sequence. These studies reported a higher recurrence of hypo-connected states in patients with SSD compared to healthy controls[16,17], and to a lesser extent in AF patients[18]. Fewer studies have examined the temporal component of such transitions. Miller and colleagues[19], for example, reported a smaller number of dFC transitions between meta-states in patients with chronic schizophrenia, and a larger similarity between meta-states, which was more pronounced in cases with more severe psychotic symptoms. A recent study examined adult patients with first episode psychosis[20], reporting higher segregation, less efficiency and greater redundancy in the flow of temporal networks. These findings were associated with antipsychotic dose and were not observed in a small group of antipsychotic naive patients.

The study of first episode AOP patients has the potential to help understand how the brain functions during rest, without the confounding effects of chronicity[19] and protracted exposure to antipsychotic medication, while focusing

on a crucial period in terms of development of brain networks. Gozdas and colleagues[21], analyzed the progression of static functional connectivity in healthy adolescents, and reported a differentiation process of spatial functional clusters, along with an enhancement of the general efficiency of the network with age. Similarly, Lopez-Vicente and colleagues[22], who specifically analyzed dFC in a sample of healthy youth, also identified an increase in the activation of the same connectivity patterns for longer periods of time over adolescence and observed that older youth spent longer time in more defined or spatially clustered meta-states. However, it remains unclear whether the onset of psychosis during adolescence can impact on physiological changes in brain network dynamics. On the other hand, grouping AOP patients according to their confirmed diagnosis over time may help dissect potentially heterogeneous pathophysiological mechanisms. Studies in AF and SSD psychoses have suggested that they present some degree of specificity in brain phenotype[16], but this has been subject to limited study and has not been examined from a dFC perspective so far[23,24].

We therefore set out to examine potential differences in the temporal component of dFC, analyzed using a graph theory approach[25], between patients with AOP divided according to diagnosis (AF vs SSD). As a secondary aim, we sought to examine whether these measures were associated with clinical characteristics of our sample, including clinical and functional severity, cannabis use and dose of anti-psychotic medication.

2. Methods

2.1. Data acquisition

Seventy-nine patients with first episode AOP aged 10 to 17 years, were recruited at the Department of Child and Adolescent Psychiatry and Psychology of the Hospital Clinic of Barcelona (Spain). Diagnosis of first episode of psychosis was established at first contact with mental health services and defined as the presence of positive psychotic symptoms of less than 12 months duration with an onset prior to age 18 (for details on baseline recruitment and assessment see[26]).

Fifty-four age-matched healthy controls (HC) were recruited within community settings from the same geographical area. General exclusion criteria were presence of autism spectrum disorders, posttraumatic stress disorders and drug-induced psychosis; intellectual disability as defined by DSM-5 criteria[27]; other neurological disorders or history of head trauma with loss of consciousness; pregnancy; and medical or technical counter-indications for MRI. Additional exclusion criteria for HC participants were a current axis I psychiatric diagnosis and having first- and second-degree relatives with any psychotic disorder[28].

The study was approved by the local Ethics Review Board. All parents or legal guardians and participants over age 12 signed informed consent or provided their assent prior to inclusion in the study. At baseline, all participants underwent a demographic and clinical assessment by experienced mental health professionals. This included the Kiddie-Schedule for Affective Disorders and Schizophrenia semi-structured interview in its Spanish version[29], administered to participants and their parents or legal guardians. The latter was repeated at 6 months follow-up to sub-divide patients into SSD (schizophrenia, schizophreniform and schizoaffective disorders) and AF (bipolar disorder or depressive disorder with psychotic symptoms), according to DSM-5 criteria[27]. Clinical severity at the time of scanning was evaluated using the Positive and Negative Syndrome Scale (PANSS)[30] and the General Assessment of Functioning (GAF) Scale. Details on current cannabis use were also recorded (categorized dichotomously as absence or presence of any use, within the 6 months prior to study intake) as well as type and dose of antipsychotic medication at the time of scanning, converted to chlorpromazine equivalents[31].

Participants also underwent a cognitive assessment with the Wechsler Intelligence Scale for Children Fourth Edition (WISCIV)[32] or Wechsler Adult Intelligence Scale–III, revised[33], when older than 16 years. Results were used to obtain their global Intelligence Quotient (gIQ) derived from the verbal comprehension and perceptual reasoning indices[34].

At intake, all participants underwent a scanning session on a 3Tesla scanner (Magnetom Trio or its upgrade, Magnetom Prismafit, Siemens, Erlangen), at the Magnetic Resonance Image Core Facility of IDIBAPS, Centre for Image Diagnosis, Hospital Clínic of Barcelona, which included a structural T1-weighted sequence, used for reference purposes, and then an 8-minute rs-fMRI acquisition with eyes closed. A technician engaged in conversation with the participants before and after the rs-fMRI session to guarantee that they did not fall asleep. Acquisition parameters were as follows: 240 volumes; TR, 2000ms; TE, 29ms; matrix size, 480*x*480; slice thickness, 4mm; acquisition matrix, 80*x*80 mm^2; 32 slices; voxel size, 3*x*3*x*4 mm^3. All MRI scans were reviewed by an experienced neuroradiologist to rule out structural pathology.

2.2. fMRI preprocessing

Raw rs-fMRI signal preprocessing is crucial for studies assessing dFC, as subject motion can bias dFC results[35]. Pre-processing for motion correction was performed based on the pipeline proposed by Parkes and colleagues[36], which is further described in *Supplement 1*.

2.3. *Network construction*

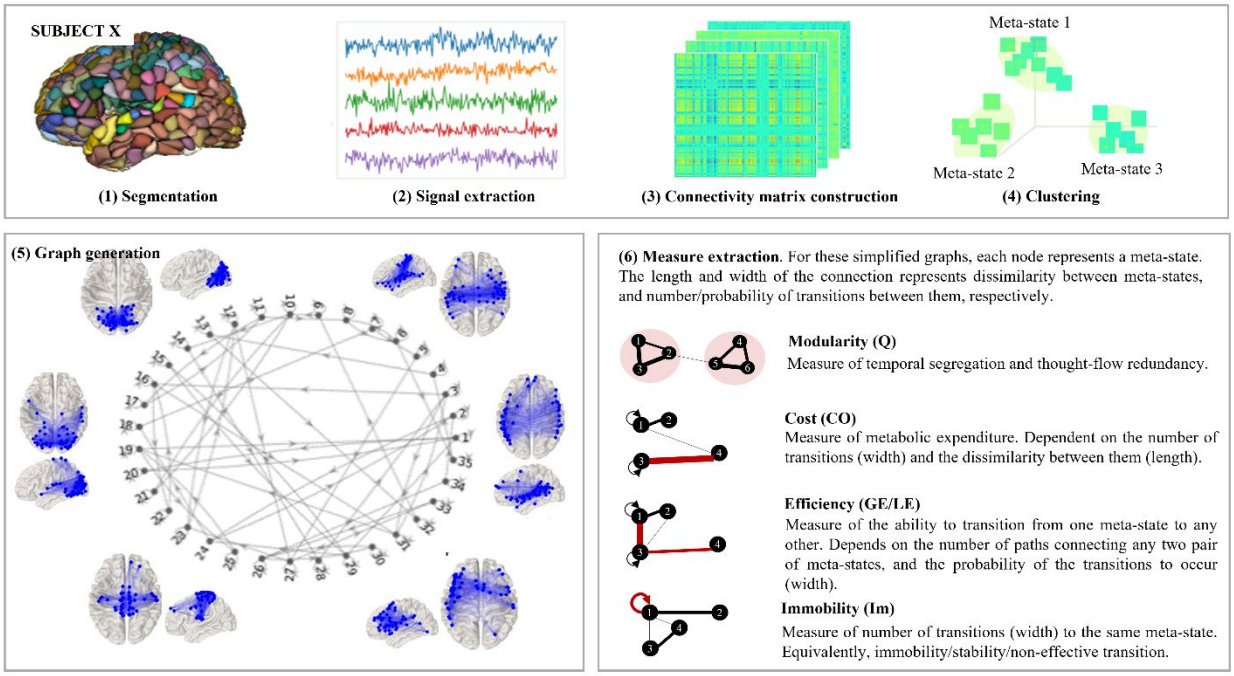

Figure 1. Scheme of the pipeline followed for each subject, and predefined number of meta-states.

To analyze dFC, directional graphs were constructed for each subject following the pipeline proposed by Ramirez-Mahaluf and colleagues[25]. Briefly, using the atlas employed by Crossley and colleagues[37], rs-fMRI signals were extracted from similarly sized regions (ROIs), which were used to generate connectivity matrices at each time step, using the Multiplication of Temporal Derivatives (MTD) [38]. These matrices were classified into more general types (i.e., meta-states) and the temporal sequence of these labels was read to generate a directed graph, providing information about how many times during the rs-fMRI the brain jumps from one specific meta-state to the others. Figure 1 schematizes this process, which is further explained in next sections.

2.3.1. *Time series extraction and connectivity matrix construction*

Pre-processed EPI volumes of each of the subjects were parceled into a total of 638 similarly sized ROIs, respecting anatomical landmarks[37], so that a time-series per region was extracted. To construct connectivity matrices, MTD[38] was the method chosen, because of its sensitivity to small variations. The main idea is that two connected regions should undergo similar changes, as opposed to those which are not. For a more robust dFC estimation, every two consecutive MTD matrices were averaged, obtaining 117 connectivity states characterized by 638 × 638-sized matrices.

2.3.2. Clustering and definition of optimal number of meta-states

MTD correlation matrices were then clustered into general types according to their similarity, using K-means. An open question when using this approach[6,39] is the number of clusters or meta-states to consider. We here propose to use a data-driven approach (*Supplement 3*), based on the idea that a specific number of meta-states is possible only if the quality of the identified meta-states is better than the one of those identified in a population of randomly generated connectivity matrices. Using this approach, we determined that the different clusters could be identified as meaningfully distinct, both for HC and AOP groups independently, only for the number of meta-states (k^n) contained in the range [5,35]. Therefore, our method identifies multiple possible sets of meta-states.

2.3.3. Transition network construction and parameter extraction

For each of the sets we constructed a graph, in order to capture how the brain temporally transitions across the set of identified whole-brain meta-states. For this purpose, labels corresponding to the cluster assigned via K-means clustering (i.e., the meta-state type), using $K=k^n$, were assigned to the sequence of connectivity matrices. This vector of labels was then consecutively read, so as to estimate the transition from meta-state activated at time t_i and its consecutive meta-state at time t_{i+1}. An adjacency matrix (A_{k^n}) was generated, of size $k^n x k^n$ (i.e., where k^n is the total number of meta-states considered), which quantifies how many times the brain transitions from the whole-brain meta-state k_i^n to k_j^n in this specific order, for each position (i,j). Each graph was constructed from A_{k^n},and used to derive the different graph measures. These included modularity (capturing redundancy and temporal segregation of the flow), immobility (capturing the extent of the absence of transitions across different meta-states), global and local efficiencies (reflecting the ability to activate the repertoire of meta-states), transition cost and leap size (a measure of metabolic expenditure and its normalization, respectively), and cost-efficiency (measuring the balance between metabolic expenditure and ability to activate all meta-states). A detailed description of these measures can be found in *Supplement 5*.

Since we ended up with several dFC descriptors estimations, one per each of the meta-state sets and subsequent graph, we reduced them into a single measure by computing the area under the curve of each of them with respect to the k^n within the feasible interval.

2.4. dFC statistical analysis

To test potential differences in extracted graph measures of AOP patients relative to HC, ANOVA tests were carried out to test the effect of group, adjusting for covariates (age, sex and frame-wise displacement, scanner model and cannabis use). Interactions between these covariates and group were also tested and were retained in the final model when significant or when variables were unequally distributed between groups. We then repeated the same analysis by further dividing AOP patients between SSD and AF.

To examine the relationship between these descriptors and clinical dimensions, general linear models (GLMs) were used to assess the effect of clinical variables (i.e. PANSS positive and negative symptoms and GAF scores; current antipsychotic dose converted to chlorpromazine equivalents; gIQ) on each graph descriptor within the whole AOP sample, adjusting for the same covariates as in the previous experiment, and controlling for the interaction of each of the clinical variables with diagnosis. We also tested the association of gIQ in both the AOP and the HC group. All p-values were corrected for multiple-comparisons using False Discovery Rate (FDR). Given an upgrade during the study period, potential scanner effects were also examined (see *Supplement 4* for details).

3. Results

3.1. Socio-demographic and Clinical Variables

Socio-demographic and clinical measures are described in Table I. The three groups did not differ in terms of age, while there was a significant difference in sex distribution between AF and SSD groups, and a trend level increase of the frame-wise displacement in AF compared to SSD patients. gIQ was significantly different across the three groups, with significantly higher scores in HC compared to both SSD and AF, but also significantly higher scores in the AF group compared to the SSD group. A trend-level higher rate of cannabis use was observed in the SSD compared to the AF group. No significant difference was found in chlorpromazine equivalents of antipsychotic dose between AOP subgroups. PANSS negative scores were significantly higher in the SSD group compared to the AF group, while there was no significant between group difference in either the PANSS positive subscale or the GAF.

	HC (N = 54)	SSD (N = 36)	AF (N = 43)	p-value	Post-hoc
Age	15.70±2.42	15.70±1.82	15.40±1.38	0.762	-
Sex (Female)	N = 27 (50.00%)	N =12 (33.30%)	N = 28 (65.10%)	0.019	SSD <AF (∗∗)
Global intelligence quotient	107±11.8	85.8±13.9	94.4±14.2	<0.001	HC >SSD (∗∗); HC >AF (∗∗); SSD <AF (∗∗)
Cannabis use	N = 8 (20.5%)	N =12 (33.3%)	N = 5 (11.6%)	0.063	SSD >AF (∗)
FD	0.09 ± 0.07	0.08±0.05	0.11±0.08	0.054	SSD <AF (∗)
Scanner (Trio)	N = 36 (83.7%)	N = 31 (86.7%)	N = 29 (69.00%)	0.121	-
Current antipsychotic dose	-	261±187	299±204	0.405	-
PANSS positive symptoms	-	19.2±4.63	20.0±7.94	0.581	-
PANSS negative symptoms	-	19.7±6.89	15.8±6.65	0.013	-
GAF	-	45.8±14.8	45.3±15.2	0.873	-

Table 1. Note: HC = Healthy Controls; SSD = Schizophrenia Spectrum Adolescent-onset First Episode Psychosis patients; AF = Affective Adolescent-onset First Episode Psychosis patients; PANSS = Positive and Negative Syndrome Scale; GAF = General Assessment of Functioning Scale; (∗∗) p<0.05; (∗) 0.09>p>0.05.

3.2. Group Comparison in dFC measures

We observed no significant differences in the dFC measurements surviving multiple comparisons correction between the entire AOP and HC. When dividing the AOP group into AF and SSD, and comparing the three groups, we found that SSD patients showed larger modularity, but reduced global efficiency in the transitions, cost, and leap size, when compared to both AF and HC groups. SSD also displayed larger immobility and decreased cost-efficiency when compared to HC. AF patients showed neither significant differences nor any trend level difference in these measures compared to HC. Estimated means and confidence intervals for the area under the curve for each of the dFC measures per group are described in Table II and figure 2. We did not find any effect of age, sex, age or sex group interaction, cannabis use, frame-wise displacement, or scanner on the findings.

	***μHC*± SE (CI 95%)**			**Statistics**	
	HC	**SSD**	**AF**	**F, corrected p-val**	**Post-hoc**
Q	4.32 ±0.067 ([4.18, 4.45])	4.58 ±0.065 ([4.45, 4.71])	4.35 ± 0.056 ([4.24,4.46])	F = 6.44 p = 0.006	*SSD* > *HC* (∗∗); p = 0.007; D = 0.76 *SSD* > *AF* (∗∗); p = 0.016; D = 0.73
GE	0.291 ±0.020 ([0.251, 0.330])	0.211 ±0.019 ([0.173,0.250])	0.273 ± 0.017 ([0.239, 0.306])	F = 6.05 p = 0.006	*SSD* < *HC* (∗∗); p = 0.007; D = -0.71 *SSD* < *AF* (∗∗); p = 0.022; D = 0.70
LE	0.731 ±0.020 ([0.690, 0.771])	0.690 ±0.020 ([0.651, 0.730])	0.725 ± 0.017 ([0.691, 0.758])	F = 1.77 p = 0.176	-
CO	170 ±8.29 ([154,187])	137 ±8.07 ([121, 153])	163 ± 6.94 ([149, 177])	F = 5.99 p = 0.006	*SSD* < *HC* (∗∗); p = 0.007; D = -0.73 *SSD* < *AF* (∗∗); p = 0.022; D = -0.64
Im	467 ±9.58 ([448, 486])	502 ±9.32 ([483, 520])	472 ± 8.02 ([456, 488])	F = 5.18 p = 0.010	*SSD* > *HC* (∗∗); p = 0.010; D = 0.54 *SSD* > *AF* (∗∗); p = 0.022; D = 0.58
LS	3.31 ±0.13 ([3.04, 3.57])	2.78 ±0.13 ([2.52, 3.04])	3.18 ± 0.11 ([2.96, 3.41])	F = 6.07 p = 0.006	*SSD* < *HC* (∗∗); p = 0.007; D = -0.82 *SSD* < *AF* (∗∗); p = 0.022; D = -0.91
CE	$[10.5 \pm 0.265]10^{-3}$ $([10.02,11.10]10^{-3})$	$[9.84 \pm 0.258]10^{-3}$ $([9.33,10.40]10^{-3})$	$[10.36 \pm 0.220]10^{-3}$ $([9.91,10.80]10^{-3})$	F = 2.75 p = 0.080	*SSD* < *HC* (∗); p = 0.050; D = -0.58

Table 2. Note: HC = Healthy Controls; SSD = Adolescent-onset First Episode Schizophrenia Spectrum Disorders; AF = Adolescent-onset First Episode Affective Psychosis patients; Q = Modularity; GE = Global Efficiency; LE = Local Efficiency; CO = Transition Cost; Im = Immobility; LS = Leap Size; CE = Cost Efficiency; μ = mean; CI = Confidence Intervals; SE = Standard Error; (∗∗) p<0.05; (∗) 0.09>p>0.05.D stands for Cohen's d.

3.3. Relationship between dFC measures and clinical characteristics

We observed no association surviving multiple-comparisons correction between any network parameter and PANSS positive or PANSS negative and GAF scores in the AOP group. Similarly, we found no significant association between gIQ and dFC measures in either the AOP or the HC group. We also observed no association between graph measures and antipsychotic doses converted to chlorpromazine equivalents, cannabis use, framewise displacement (see also table S1.1 *Supplement 1*) or scanner.

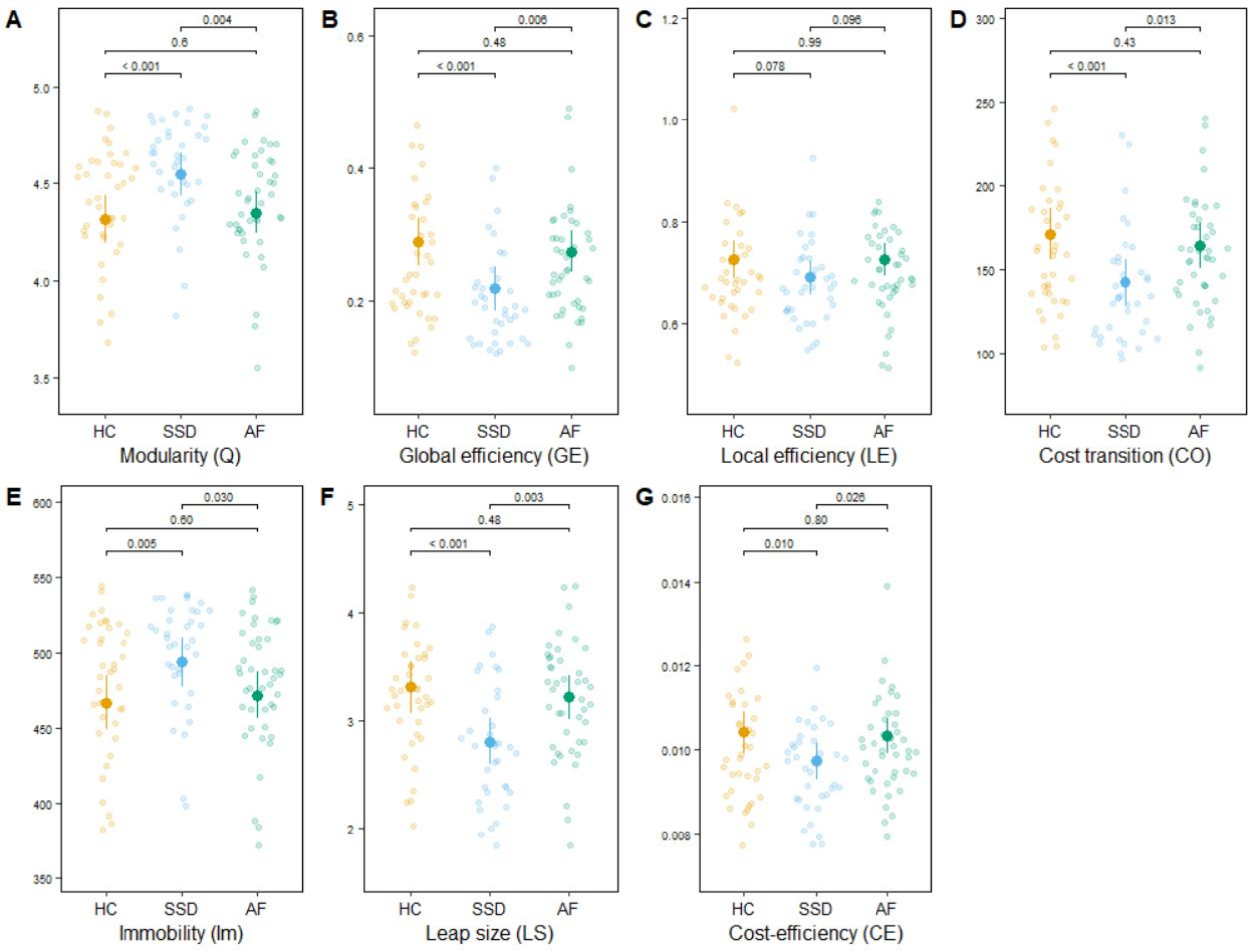

Figure 2. Estimated means and confidence intervals for the area under curve of each of the dynamic measures per group: HC (healthy controls, yellow), SSD (schizophrenia spectrum disorder AOP, blue) and AF (affective AOP, green). Uncorrected p-values for each group comparison are shown in each graph.

4. Discussion

In the present study, we initially compared whole-brain dFC between AOP and HC groups and observed no significant differences. When dividing the AOP group based on diagnosis, we observed changes in patients with SSD relative to both patients with AF and HC. Our results suggest that at illness onset, SSD patients showed greater redundancy in temporal trajectories, reflected through greater modularity in the flow between meta-states, and longer periods of immobility. We also identified greater difficulty in activating the full repertoire of possible meta-states, as reflected by reduced global efficiency. These changes were observed alongside alterations in measures associated with metabolism, as we found a decrease in the global metabolic demands and in those only associated with transitions. This not only suggests that there is a reduction in metabolic expenditure due to increased immobility rates, but also due to such transitions predominantly occurring between more similar meta-states. It is worth noting that the described measures are highly correlated, and from the graph theory perspective, an optimal increase in the modularity with a subsequent decrease in the global efficiency could lead to a favorable decrease of the metabolic demands. The ability to equally transition from one meta-state to any other may come with larger metabolic demands, especially if the meta-states involved are very dissimilar. Assigning a larger probability to transitions between more similar meta-states may come with conveniently lower metabolic demands, so that the brain would be transitioning in a cost-efficient manner[44]. In fact, Ramirez-Mahaluf and colleagues[25] reported a positive association between cost-efficiency of transitions and gIQ in HC, confirming that networks displaying abnormal dFC may still be cost-efficient. However, in our study, this was not the case for SSD participants, who also displayed reduced cost-efficiency when compared to HC, confirming that these alterations reflect actual impairments. These results are consistent with dFC findings in a sample of adult patients with chronic schizophrenia[19], and recently, in a first episode psychosis sample[20]. Thus, our results further support the idea that these changes are already present at the beginning of the clinical course of the disease[2].

In contrast with the SSD group and contrary to our prediction, we found no evidence of significant dFC alterations in AF patients compared to HC. AF patients differed from SSD patients by displaying preserved dynamic fluidity (immobility), a greater variety in mental transitions (modularity) and an associated higher metabolic expenditure (cost and leap size). Previous studies in chronic patients reported that AF patients displayed intermediate alterations between patients with SSD and HC[18]. This contrasts with our findings and raises the possibility that dFC abnormalities in AF patients may manifest later over the course of disease. Such possibility would be in keeping with the suggestion that neurodevelopmental mechanisms are more pronounced in the pathophysiology of SSD compared to AF[45] but would need to be tested systematically in a sample of patients assessed at different illness stages.

Of particular interest is the relationship between antipsychotic treatment and dFC measures. Previously, Lottman and colleagues[46] examined dFC in first-episode patients with schizophrenia while unmedicated and after 6 weeks of treatment, describing the dwell and fraction of time spent in differently connected general meta-states. They found that before treatment, patients with schizophrenia tended to spend less time in poorly connected meta-states than HC, but such dwell time stabilized after treatment. The authors tentatively attributed the initial reduction of time in hypoconnected meta-states to glutamatergic hyperactivity that stabilized after treatment. This hypothesis could also apply to our findings for SSD. In fact, Ramirez-Mahaluf and colleagues[20] reported in their adult FEP sample, which predominantly included SSD patients, similar findings to those in our SSD group, and an association between such measures and dose of antipsychotic treatment.

However, in our sample, which had received lower doses of antipsychotic treatment, we did not observe this association. Furthermore, while doses of medication were statistically equivalent between SSD and AF groups, we only observed dFC impairments in SSD participants. Our results therefore extend the findings by Ramirez-Mahaluf and colleagues[20] and Lottman and colleagues[46], by suggesting that changes in dFC in SSD patients with first episode psychosis with an onset during adolescence are unlikely to be simply an epiphenomenon of antipsychotic treatment.

Consistent with Ramirez-Mahaluf and colleagues[20], we observed no significant association between dFC descriptors and gIQ in AOP. However, contrary to our prediction, we failed to observe this association in the HC group, which was previously reported in a study[25] using a composite cognitive measure obtained via principal component analysis. This methodological difference may partially explain the difference in the results. The gIQ may sub-optimally characterize the variability present in our sample when compared to a composite measure tailored to the sample. This could also suggest that dFC descriptors could correlate differently to each of the original cognitive dimensions. We also observed no significant association between dFC descriptors and measures of clinical severity. Taken together, our results might suggest that dFC measures may perform better at capturing underlying pathophysiological mechanisms, rather than directly reflecting specific clinical or cognitive domains. In view of the results and to understand what these particular dFC measurements represent, future studies should focus on their correlation with measures closer to pathophysiology, such as neurometabolites, and/or structural and effective connectivity.

Several methodological considerations need to be acknowledged when interpreting the findings of this study. First, we cannot rule out that the lack of case-control findings in AF or the association of dFC measures to clinical and

demographical measures is due to insufficient power to detect small effects. A larger sample size per group would help to interpret our findings. Second, the choice of method for analyzing rs-fMRI data may have influenced our results: unlike other approaches, this method is able to capture changes that take place in the temporal dimension of rs-fMRI; however, these are also summarized in mean measures which span across time and structures. This can be advantageous, as it enables to easily describe a structure that is organized in the form of a complex network; however, average measures may also mask other biologically relevant information. It is also important to acknowledge that there are various approaches to dFC analysis in the literature which follow different methodological choices throughout the pipeline, ranging from the definition of the regions from which to extract the BOLD signal, to the method to compute and identify the different connectivity patterns and meta-states. One of the strengths of our study is the data-driven choice of the number of meta-states. However further studies should be carried out to quantify the influence of other methodological decisions on the quality and robustness of the result. Finally, we chose to focus on a sample that was clinically representative of youth with a first episode of psychosis, therefore use of cannabis was not an exclusion criterion, although drug-induced psychosis was. There was a sex imbalance between patient groups, which is consistent with an earlier age onset of SSD in males, while all analyses included sex as covariate and no sex effects were detected. Patients had a recent onset of the disease and had received overall a short exposure to medication, although we examined the effect of antipsychotic medication quantitatively to measure its effects on our findings. It is extremely challenging to scan adolescents with a first episode of psychosis naïve to antipsychotic (or other sedative) medications and is not an option in our clinical setting.

To conclude, during rest, adolescents with SSD transitioned between mental meta-states in a less random manner and with reduced metabolic cost relative to HC, possibly reflecting inefficiency in the activation of different connectivity patterns. These alterations are already present at illness onset, are not likely to be simply an epiphenomenon of antipsychotic treatment, and are independent of clinical severity, suggesting that a combination of the described dFC measures holds potential as a brain-based biomarker, specifically characterizing youth with SSD.

5. Acknowledgements

IB received support from Angelini, as GS and DI, Otsuka-Lundbeck and Janssen, and grants from the Spanish Ministry of Health, Instituto de Salud Carlos III supported by ERDF Funds from the European Commission (PI18/0242/PI21/0391). GS also received grants from the Spanish Ministry of Health, Instituto de Salud Carlos III supported by ERDF Funds from the European Commission (PI18/00976; 21/00330), the Alicia Koplowitz Foundation,

the Fundació Clínic Recerca Biomèdica and Brain and Behavior Research Foundation (NARSAD Young Investigator Award 26731). GP is supported by ICREA Academia programme. The remaining authors declare no conflicts of interest. This work has been performed thanks to the 3T Equipment of Magnetic Resonance at IDIBAPS (project IBPS15-EE-3688 cofounded by MCIU and by ERDF). The funding sources had no role in study design, interpretation of results, report writting or in the decision to submit the article for publication. We would like to thank Roger Borras[c].

6. References

1. Castro-Fornieles J, Baeza I, de la Serna E, et al. Two-year diagnostic stability in adolescent-onset first-episode psychosis. *J Child Psychol Psychiatry*. 2011;52(10):1089-1098. doi:10.1111/j.1469-7610.2011.02443.x

2. Driver DI, Thomas S, Gogtay N, Rapoport JL. Childhood-Onset Schizophrenia and Adolescent-onset Schizophrenia Spectrum Disorders. *Child Adolesc Psychiatr Clin N Am*. 2020;29(1):71-90. doi:10.1016/j.chc.2019.08.017

3. Friston K, Brown HR, Siemerkus J, Stephan KE. The dysconnection hypothesis (2016). *Schizophr Res*. 2016;176(2-3):83-94. doi:10.1016/j.schres.2016.07.014

4. Thompson GJ. Neural and metabolic basis of dynamic resting state fMRI. *Neuroimage*. 2018;180:448-462. doi:10.1016/j.neuroimage.2017.09.010

5. Rotarska-Jagiela A, van de Ven V, Oertel-Knöchel V, Uhlhaas PJ, Vogeley K, Linden DEJ. Resting-state functional network correlates of psychotic symptoms in schizophrenia. *Schizophr Res*. 2010;117(1):21-30. doi:10.1016/j.schres.2010.01.001

6. O'Neill A, Carey E, Dooley N, et al. Multiple Network Dysconnectivity in Adolescents with Psychotic Experiences: A Longitudinal Population-Based Study. *Schizophr Bull*. 2020;46(6):1608-1618. doi:10.1093/schbul/sbaa056

7. Li S, Hu N, Zhang W, et al. Dysconnectivity of Multiple Brain Networks in Schizophrenia: A Meta-Analysis of Resting-State Functional Connectivity. *Front Psychiatry*. 2019;10. doi:10.3389/fpsyt.2019.00482

8. Zhao X, Wu Q, Chen Y, Song X, Ni H, Ming D. Hub Patterns-Based Detection of Dynamic Functional Network Metastates in Resting State: A Test-Retest Analysis. *Front Neurosci*. 2019;13. doi:10.3389/fnins.2019.00856

9. Rikandi E, Mäntylä T, Lindgren M, Kieseppä T, Suvisaari J, Raij TT. Functional network connectivity and topology during naturalistic stimulus is altered in first-episode psychosis. *Schizophr Res*. 2022;241:83-91. doi:10.1016/j.schres.2022.01.006

10. Lord L-D, Allen P, Expert P, et al. Functional brain networks before the onset of psychosis: A prospective fMRI study with graph theoretical analysis. *NeuroImage Clin*. 2012;1(1):91-98.

doi:10.1016/j.nicl.2012.09.008

11. Cao H, Ingvar M, Hultman CM, Cannon T. Evidence for cerebello-thalamo-cortical hyperconnectivity as a heritable trait for schizophrenia. *Transl Psychiatry*. 2019;9(1):192. doi:10.1038/s41398-019-0531-5

12. Chang C, Glover GH. Time–frequency dynamics of resting-state brain connectivity measured with fMRI. *Neuroimage*. 2010;50(1):81-98. doi:10.1016/j.neuroimage.2009.12.011

13. Deco G, Ponce-Alvarez A, Mantini D, Romani GL, Hagmann P, Corbetta M. Resting-State Functional Connectivity Emerges from Structurally and Dynamically Shaped Slow Linear Fluctuations. *J Neurosci*. 2013;33(27):11239-11252. doi:10.1523/JNEUROSCI.1091-13.2013

14. Cabral J, Kringelbach ML, Deco G. Functional connectivity dynamically evolves on multiple time-scales over a static structural connectome: Models and mechanisms. *Neuroimage*. 2017;160:84-96. doi:10.1016/j.neuroimage.2017.03.045

15. Rashid B, Arbabshirani MR, Damaraju E, et al. Classification of schizophrenia and bipolar patients using static and dynamic resting-state fMRI brain connectivity. *Neuroimage*. 2016;134:645-657. doi:10.1016/j.neuroimage.2016.04.051

16. Du Y, Pearlson GD, Yu Q, et al. Interaction among subsystems within default mode network diminished in schizophrenia patients: A dynamic connectivity approach. *Schizophr Res*. 2016;170(1):55-65. doi:10.1016/j.schres.2015.11.021

17. Damaraju E, Allen EA, Belger A, et al. Dynamic functional connectivity analysis reveals transient states of dysconnectivity in schizophrenia. *NeuroImage Clin*. 2014;5:298-308. doi:10.1016/j.nicl.2014.07.003

18. Du Y, Pearlson GD, Lin D, et al. Identifying dynamic functional connectivity biomarkers using GIG-ICA: Application to schizophrenia, schizoaffective disorder, and psychotic bipolar disorder. *Hum Brain Mapp*. 2017;38(5):2683-2708. doi:10.1002/hbm.23553

19. Miller RL, Yaesoubi M, Turner JA, et al. Higher Dimensional Meta-State Analysis Reveals Reduced Resting fMRI Connectivity Dynamism in Schizophrenia Patients. *PLoS One*. 2016;11(3):e0149849. doi:10.1371/journal.pone.0149849

20. Ramirez-Mahaluf JP, Tepper Á, Alliende LM, et al. Dysconnectivity in Schizophrenia Revisited: Abnormal Temporal Organization of Dynamic Functional Connectivity in Patients With a First Episode of Psychosis. *Schizophr Bull*. December 2022. doi:10.1093/schbul/sbac187

21. Gozdas E, Holland SK, Altaye M. Developmental changes in functional brain networks from birth through adolescence. *Hum Brain Mapp*. 2019;40(5):1434-1444. doi:10.1002/hbm.24457

22. López-Vicente M, Agcaoglu O, Pérez-Crespo L, et al. Developmental Changes in Dynamic Functional Connectivity From Childhood Into Adolescence. *Front Syst Neurosci*. 2021;15. doi:10.3389/fnsys.2021.724805

23. Zhong Y, Wang C, Gao W, et al. Aberrant Resting-State Functional Connectivity in the Default Mode Network in Pediatric Bipolar Disorder Patients with and without Psychotic Symptoms. *Neurosci Bull*. 2019;35(4):581-590. doi:10.1007/s12264-018-0315-6

24. Hilland E, Johannessen C, Jonassen R, et al. Aberrant default mode connectivity in adolescents with adolescent-onset psychosis: A resting state fMRI study. *NeuroImage Clin*. 2022;33:102881. doi:10.1016/j.nicl.2021.102881

25. Ramirez-Mahaluf JP, Medel V, Tepper Á, et al. Transitions between human functional brain networks reveal complex, cost-efficient and behaviorally-relevant temporal paths. *Neuroimage*. 2020;219:117027. doi:10.1016/j.neuroimage.2020.117027

26. Castro-Fornieles J, Parellada M, Gonzalez-Pinto A, et al. The child and adolescent first-episode psychosis study (CAFEPS): Design and baseline results. *Schizophr Res*. 2007;91(1-3):226-237. doi:10.1016/j.schres.2006.12.004

27. *Diagnostic and Statistical Manual of Mental Disorders, IV-TR*. 157th ed.; 2000.

28. Ilzarbe D, de la Serna E, Baeza I, et al. The relationship between performance in a theory of mind task and intrinsic functional connectivity in youth with early onset psychosis. *Dev Cogn Neurosci*. 2019;40:100726. doi:10.1016/j.dcn.2019.100726

29. Ulloa RE Higuera F, Nogales I, Fresán A, Apiquian R, Cortés J, Arechavaleta B, Foulliux C, Martínez P, Hernández L, Domínguez E, de la Peña F OS. Estudio de fiabilidad interevaluador de la versión en español de la entrevista Schedule for Affective Disorders and Schizophrenia for School-Age Children--Present and Lifetime version (K-SADS-PL). *Actas Esp Psiquiatr*. 2006;34(1):36-40.

30. Kay SR, Fiszbein A, Opler LA. The Positive and Negative Syndrome Scale (PANSS) for Schizophrenia. *Schizophr Bull*. 1987;13(2):261-276. doi:10.1093/schbul/13.2.261

31. Leucht S, Samara M, Heres S, Davis JM. Dose Equivalents for Antipsychotic Drugs: The DDD Method: Table 1. *Schizophr Bull*. 2016;42(suppl 1):S90-S94. doi:10.1093/schbul/sbv167

32. Wechsler D. *WISC-R Escala de Inteligencia de Wechsler Para Niños - Revisada*. 9th ed. TEA; 2001.

33. Wechsler D. *Wechsler Abbreviated Scale of Intelligence WASI: Manual*. 4th ed. Pearson/PsychCorpl; 1999.

34. Flanagan DP, Alfonso VC. *Essentials of WISC-V Assessment*. Vol 1. John Wiley & ons; 2017.

35. Power JD, Schlaggar BL, Petersen SE. Recent progress and outstanding issues in motion correction in resting state fMRI. *Neuroimage*. 2015;105:536-551. doi:10.1016/j.neuroimage.2014.10.044

36. Parkes L, Fulcher B, Yücel M, Fornito A. An evaluation of the efficacy, reliability, and sensitivity of motion correction strategies for resting-state functional MRI. *Neuroimage*. 2018;171:415-436. doi:10.1016/j.neuroimage.2017.12.073

37. Crossley NA, Mechelli A, Vértes PE, et al. Cognitive relevance of the community structure of the human brain functional coactivation network. *Proc Natl Acad Sci*. 2013;110(28):11583-11588. doi:10.1073/pnas.1220826110

38. Shine JM, Koyejo O, Bell PT, Gorgolewski KJ, Gilat M, Poldrack RA. Estimation of dynamic functional connectivity using Multiplication of Temporal Derivatives. *Neuroimage*. 2015;122:399-407. doi:10.1016/j.neuroimage.2015.07.064

39. Núñez P, Poza J, Gómez C, et al. Abnormal meta-state activation of dynamic brain networks across the Alzheimer spectrum. *Neuroimage*. 2021;232:117898. doi:10.1016/j.neuroimage.2021.117898

40. Newman MEJ. Modularity and community structure in networks. *Proc Natl Acad Sci*. 2006;103(23):8577-8582. doi:10.1073/pnas.0601602103

41. Blondel VD, Guillaume J-L, Lambiotte R, Lefebvre E. Fast unfolding of communities in large networks. *J Stat Mech Theory Exp*. 2008;2008(10):P10008. doi:10.1088/1742-5468/2008/10/P10008

42. Latora V, Marchiori M. Efficient Behavior of Small-World Networks. *Phys Rev Lett*. 2001;87(19):198701. doi:10.1103/PhysRevLett.87.198701

43. Fornito A, Zalesky A, Bassett DS, et al. Genetic Influences on Cost-Efficient Organization of Human Cortical Functional Networks. *J Neurosci*. 2011;31(9):3261-3270. doi:10.1523/JNEUROSCI.4858-10.2011

44. Zalesky A, Fornito A, Cocchi L, Gollo LL, Breakspear M. Time-resolved resting-state brain networks. *Proc Natl Acad Sci*. 2014;111(28):10341-10346. doi:10.1073/pnas.1400181111

45. Valli I, Serna ED La, Borràs R, et al. Cognitive heterogeneity in the offspring of patients with schizophrenia or bipolar disorder: a cluster analysis across family risk. *J Affect Disord*. 2021;282(November 2020):757-765. doi:10.1016/j.jad.2020.12.090

46. Lottman KK, Kraguljac N V., White DM, et al. Risperidone Effects on Brain Dynamic Connectivity—A Prospective Resting-State fMRI Study in Schizophrenia. *Front Psychiatry*. 2017;8. doi:10.3389/fpsyt.2017.00014

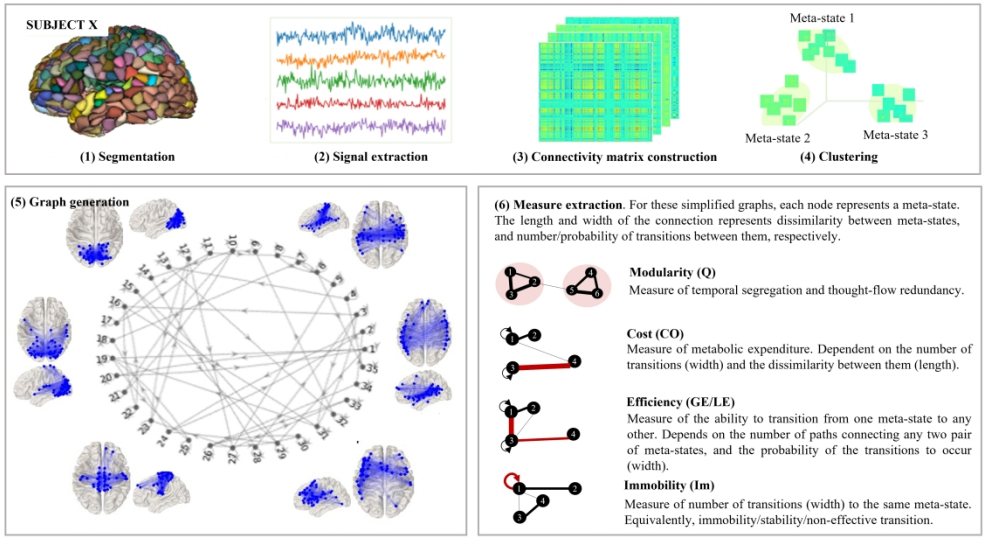

Scheme of the pipeline followed for each subject, and predefined number of meta-states.

819x457mm (130 x 130 DPI)

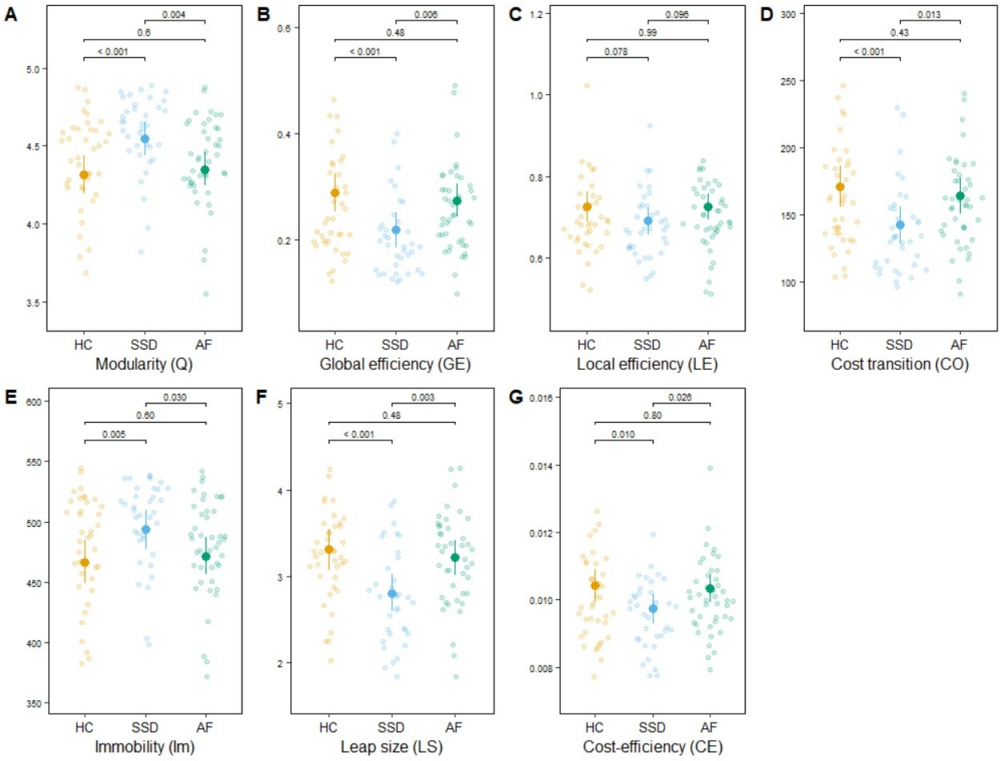

Estimated means and confidence intervals for the area under curve of each of the dynamic measures per group: HC (healthy controls, yellow), SSD (schizophrenia spectrum disorder AOP, blue) and AF (affective AOP, green). Uncorrected p-values for each group comparison are shown in each graph.

264x201mm (120 x 120 DPI)

Supplemental material for: Altered temporal dynamics of resting-state fMRI in adolescent-onset first-episode psychosis

Contents

Supplement 1. fMRI preprocessing

Raw rs-fMRI signal preprocessing is crucial for studies assessing dFC, as subject motion can bias dFC results[1]. Several denoising methods have been proposed in the literature to mitigate motion-related artifacts in fMRI, including regression of head motion parameters, and physiological signals, aCompCor method, ICA-AROMA and censoring strategies. Parkes and colleagues[2] investigated the effectiveness and robustness of these different denoising methods and their possible combinations and concluded that both ICA-AROMA and censoring strategies were the most successful in the mitigation of motion-related artifacts. While censoring strategies were the most effective between the two, they were associated with a greater loss of temporal degrees of freedom, which is an especially relevant feature in our study where we are specifically interested in the temporal component of the signal. ICA-AROMA, on the other hand, was in general only marginally inferior to censoring strategies, and was the one providing the most robust results in different combinations with the other mentioned denoising techniques.

For all the aforementioned reasons, in this study we employed the ICA-AROMA based strategy, in combination with regression of head motion parameters (i.e., 24), and physiological signals (i.e., white matter and cerebrospinal fluid signal), with the exclusion of subjects using lenient criteria, given the modest sample size.

In detail, subject motion was reported through Framewise Displacement (FD), excluding all patients displaying a mean FD > 0.55mm. Then, the T1-weighted MRI was subjected to neck cropping, followed

by N4 bias-field correction and tissue segmentation. For the rs-fMRI sequence, the first four volumes were excluded, while the rest were slice-time corrected and realigned, first to the first volume and then to the mean. The realigned images were co-registered rigidly to native T1, and the T1 image was spatially normalized to MNI space. This transformation was applied to the corrected EPI volumes and T1-derived tissue masks. Linear de-trending of the BOLD time series, intensity normalization of the EPI data to 1000-unit mode, spatial smoothing using a 6mm Gaussian full-width at half-maximum kernel, and bandpass filtering between 0.008 and 0.08 Hz using fast Fourier transform were performed. Residual motion was addressed using the ICA-AROMA denoising method[3] and corrected masks of the white matter and cerebrospinal fluid were used to estimate mean trends caused by head motion and physiological fluctuations of non-neural origin, which were then regressed out. MATLAB R2020a, SPM12 and ANTs were used for the whole pipeline.

To check the quality of the preprocessing steps, we computed QC-dFC correlations. We assessed Pearson's correlation coefficients between the original FD and the dFC parameters extracted from the corrected sequences. The results (S1.1.) suggest that after correction there is no statistically significant linear correlation between the originally calculated FD and the extracted dFC measures. This is in agreement with the results of Parkes et al.[2] using the same pipeline. However, and as explained in section *2.4.*, FD was subsequently used as a regressor to account for possible residual effects in all models.

	Pearson's r	**CI 95%**	**t-statistic**	**p.value (uncorrected)**
FD-Q	-0.06	[-0.22, 0.11]	-0.70	0.49
FD-GE	0.05	[-0.12, 0.21]	0.60	0.56
FD-LE	-0.07	[-0.24, 0.11]	-0.80	0.43
FD-CO	0.06	[-0.11, 0.23]	0.74	0.46
FD-Im	-0.05	[-0.22, 0.12]	-0.56	0.58
FD-LS	0.08	[-0.09, 0.25]	0.93	0.35
FD-CE	0.01	[-0.16, 0.18]	0.17	0.87

Table S 1.1. QC-FC Pearson's correlation coefficient, as a measure of the residual effect of in-scanner motion (FD) on dFC measures after noise correction. The significance of the correlation was tested using t-statistic.

Supplement 2. Multiplication of Temporal Derivatives

To generate the initial set of temporal connectivity patterns from rs-fMRI, Multiplication of Temporal Derivatives (MTD) was performed[4]. The main idea behind this method is that connected regions should vary similarly at each time point. To do so, for each node i, and for each time t, the method computes the normalized temporal derivative dt_{it}, as well as its variability $\sigma_{i,}$ along the whole acquisition period. Then, the functional coupling between pairs of nodes per time step is estimated as the product of the respective pairs of normalized temporal derivatives, as follows:

$$MTD_{ijt} = \frac{dt_{it} \cdot dt_{jt}}{\sigma_i \cdot \sigma_j}$$

The rs-fMRI sequence leads to a matrix of size 235 time-points × 638 × 638 ROIs. This method was chosen over other approaches because of its superior sensitivity to small variations. One of the limitations of dFC analyses is that it is difficult to assess whether a large functional covariance between regions is caused by genuine synchronization or due to stochasticity of rs-fMRI signal. However, Shine and colleagues[4] demonstrated that this method outperformed classical sliding-window approaches in detecting small variations, while being robust after averaging the MTD using small sliding windows. Therefore, for a more robust estimation of co-variance, the resulting MTD matrix was averaged through the first dimension using a simple moving window length of 2 volumes.

Supplement 3. Definition of the optimal number of meta-states

Prior to the construction of the directed graph, Multiplication of Temporal Derivatives (MTD) correlation matrices were clustered into general connectivity pattern types according to their similarity, using K-means. An open question when using this approach[5,6] is the number of clusters or meta-states to consider. While some authors advocate for the use of a small number of meta-states, others consider that this number may depend on the recording period[7] and have proposed the use of wider intervals, in some cases lacking quantitative validation. Besides, it is important to note that ours is a younger sample, and the degree of maturity of brain networks may play a role in the plausible number of meta-states that can be considered. Here we propose a data-driven approach to address this issue.

We suggest that we cannot define a unique number of meta-states, since the different connectivity matrices are likely to lie in a continuous distribution in the correlation space. By considering fewer meta-states we would be describing more general connectivity patterns, while by considering a larger number of meta-states we would be describing more precise patterns. Nevertheless, we suggest that there is a limit in the plausible number of meta-states, which is when the quality of the identified clusters (or meta-states) is no different than the quality of clusters identified in a random distribution. Beyond this point, we cannot guarantee that the identified meta-states are meaningfully different, and therefore some transitions in the derived graphs could be meaningless.

To determine the optimal K set (i.e., number of possible clusters), a projection-based clustering approach was adopted. Specifically, for each subject within the healthy control (HC) group, the Uniform Manifold Approximation and Projection[8] *(UMAP)* was used to find a low dimensional embedding of their connectivity matrices, which had an original size of 203,203 variables (i.e., considering only the upper-diagonal part of the symmetric connectivity matrices). In this low dimensional space, the 117 connectivity matrices were clustered, using k-means with all k^n values within the range [5,95]. The quality of the clustering per k^n was assessed using Silhouette score[9]. The process was repeated for all subjects within the HC group, so a distribution of Silhouette scores per k^n for the whole HC group was obtained. Then, this same process was run on 117 randomly generated connectivity matrices, an experiment repeated N times (where N is the number of subjects within the HC group), yielding an equivalent distribution of Silhouette scores per k^n for all generated null models. In all cases, parameters for UMAP were 10 neighbors and a minimum distance of 0.3; whereas K-means was performed using $2 \cdot 10^4$ replicates. Both distributions were

then plotted using boxplots per k^n, as depicted in *figure S2.1.*, which revealed that only in range [5,35] the interquartile range of both distributions did not overlap. Our interpretation is that this was the only range where the different clusters could be identified as meaningfully separated clusters for our HC participants.

Based on previous literature[10,11] ,we hypothesized that the number of significantly different meta-states may not necessarily be the same for the psychosis sample. Therefore, the same experiment was independently performed for the AOP sample, which revealed the same difference in the Silhouette scores within the range [5,35].

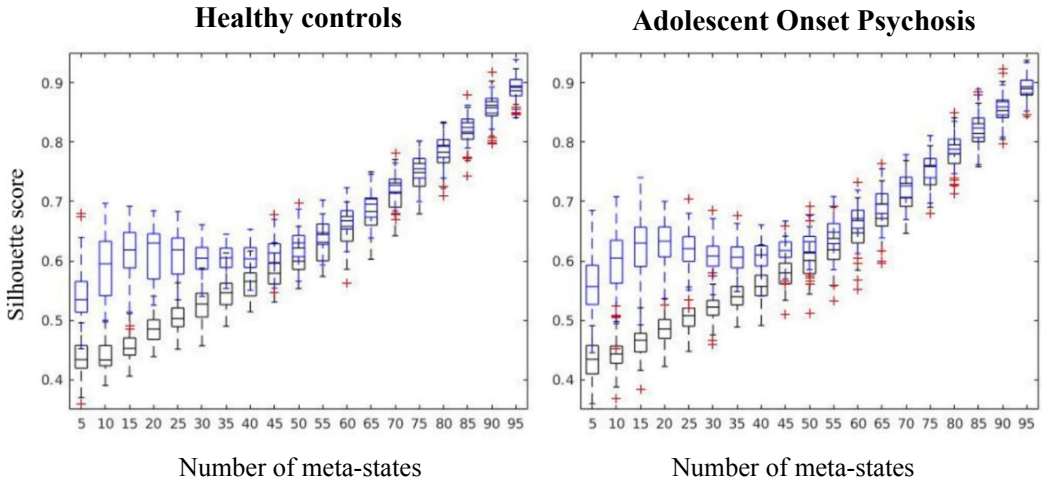

Figure S3.1. Distribution of Silhouette scores per k^n clusters of connectivity matrices in a reduced space, both for healthy controls and first episode psychosis patients (blue), compared to that of null models (black).

Supplement 4. Group comparison in dFC measures, using rs-fMRI from single scanner

During the acquisition period there was an upgrade of the scanner which was used to acquire rs-fMRI sequences, from *MAGNETOM Trio* (Siemens Healthcare, Erlangen, Germany) to *MAGNETOM Prisma*^{fit}, from the same manufacturer. *Siemens Healthcare* stated that the upgrade was neither intended to improve quality or stability of the EPI-BOLD scanning, nor they found any relevant differences in the BOLD signal when using standard scanning routines[12], which is the case of the current study.

However, this variable was considered as a potential confounding factor of the model when testing the effect of group (SSD vs AF vs HC) in the extracted dFC measures in this study. As mentioned in section 3.1 and 3.2 of the main text, we found no significant difference in the distribution of the scanner used for the acquisition of the rs-fMRI sequences per group, and we did not find a significant effect of the scanner type in the resulting model. For all the above reasons, in the main text, we reported dFC measures' differences using data extracted from both scanners. Figure S3.1. displays the estimated means and confidence intervals for each of the measures, divided by groups (i.e., HC, SSD, and AF) and scanner(i.e., *MAGNETOM Trio*, T; and *MAGNETOM Prisma*^{fit}, P).

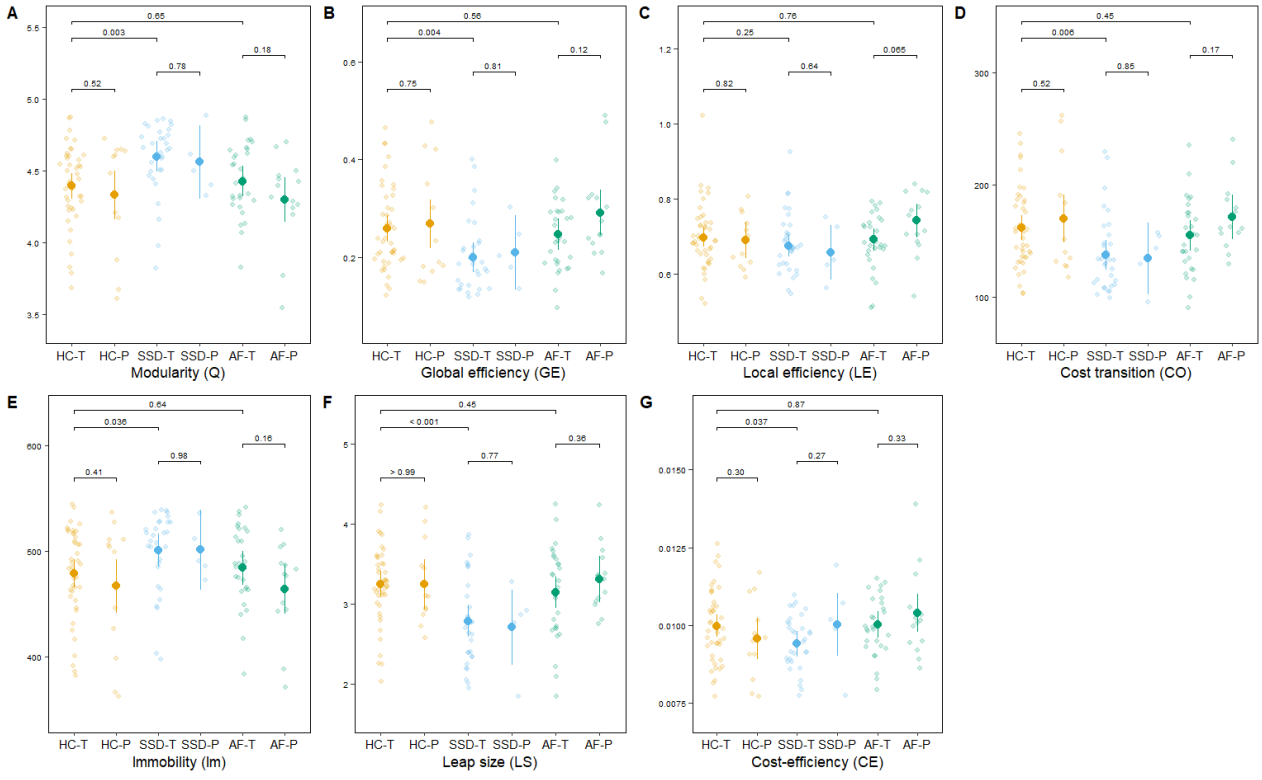

Figure S4 1. Estimated means and confidence intervals for the area under curve of each of the dynamic measures per group, in the subgroup of subjects scanned at the MAGNETOM Trio (T) scanner and its upgrade Prisma^{Fit} *(P): HC (healthy controls, yellow), SSD (schizophrenia spectrum disorder AOP, blue), and AF (affective AOP, green). Uncorrected p-values for each group comparison are shown in each graph.*

Note that the sample scanned using MAGNETOM Prisma^{fit} is modest, with N^{HC}_P = 12, N^{SSD}_P = 5, N^{AF}_P=14, so we can neither statistically confirm nor disprove any bias within each of the groups. Therefore, in this section we further tested the effect of group on dFC measures, by using only data from the most frequently used scanner throughout the acquisition of the sample (*MAGNETOM* Trio, Siemens, Erlangen, Germany).

The characteristics of this sub-sample are further described in table S1. Similar to the whole sample, there were no statistically significant differences in the distribution of age across groups, or on cannabis use. The differences in sex distribution between AF and SSD group remained, with a larger percentage of females in the AF group. We also found a trend-level increase in frame-wise displacement in the AF group with respect to HC.

	HC (N = 36)	**SSD (N = 31)**	**AF (N = 29)**	**p.value**	**Post-hoc**
Age	15.20±1.89	15.80±1.73	15.20±1.46	0.309	-
Sex (Female)	N = 21 (58.30%)	N =11 (35.50%)	N = 21 (72.4.10%)	0.014	SSD <AF (∗∗)
Cannabis use	N = 7 (20.6%)	N =11 (35.3%)	N = 4 (13.8%)	0.124	-
FD	0.07 ± 0.03	0.07±0.04	0.10±0.08	0.052	HC <AF (∗)

Table S 4.1. Note: HC = Healthy Controls; SSD = Schizophrenia Spectrum Adolescent-Onset First-Episode Psychosis patients; AF = Affective Adolescent-Onset First-Episode Psychosis patients; (**) p<0.05; (*) 0.09>p>0.05

We then performed an ANOVA using the subgroup of patients scanned at *MAGNETOM* Trio, adjusting for the remaining covariates (age, sex, frame-wise displacement, and cannabis use), and controlling for interactions of these covariates with sub-group when unequally distributed. The new results are further described in Table S3.2 and can be seen in Figure S3.1.

As in the first experiment reported in the paper, we found that the SSD group showed a statistically greater modularity and immobility, but reduced global efficiency, metabolic cost and leap size compared to HC. With regards to AF, SSD patients showed a trend-level decrease in leap size, which did not reach significance possibly due to a reduction of the sample size. Nevertheless, these results, added to the fact that we did not find a scanner effect in the original model, further help confirm that these changes are associated with disease and independent of scanner.

	***μHC*± SE (CI 95%)**			**Statistics**	
	HV	**SSD**	**AF**	**F, corrected p-val**	**Post-hoc**
Q	4.37 ± 0.050 ([4.27, 4.47])	4.60 ± 0.050 ([4.50, 4.70])	4.44 ± 0.060 ([4.32,4.56])	F =5.83 p = 0.012	SSD > HC (∗∗); p = 0.009; Cd = 0.83
GE	0.272 ± 0.015 ([0.242, 0.303])	0.202 ± 0.015 ([0.172,0.233])	0.245±0.0184 ([0.208, 0.281])	F = 5.57 p = 0.012	SSD < HC (∗∗); p = 0.009; Cd = -0.80
LE	0.718 ± 0.016 ([0.685, 0.751])	0.681±0.017 ([0.648, 0.714])	0.690±0.020 ([0.650, 0.729])	F = 0.92 p = 0.403	-
CO	166 ± 6.70 ([153,180])	137±6.74 ([124, 151])	152±8.04 ([136, 168])	F = 4.87 p = 0.017	SSD < HC (∗∗); p = 0.015; Cd = -0.73
Im	472 ± 7.69 ([457, 488])	501±7.74 ([485, 516])	487±9.22 ([468, 505])	F = 3.31 p = 0.056	SSD > HC (∗); p = 0.064; Cd = 0.58
LS	3.28 ± 0.106 ([3.07, 3.49])	2.77±0.106 ([2.56, 2.98])	3.13±0.127 ([2.88, 3.38])	F = 6.61 p = 0.012	SSD < HC (∗∗); p = 0.007; Cd = -0.89 SSD < AF (∗); p = 0.066; Cd = -0.65
CE	$[10.19\pm 0.200] \cdot 10^{-3}$ $([9.79,10.59]10^{-3})$	$[9.53 \pm 0.201] \cdot 10^{-3}$ $([9.13,9.93]10^{-3})$	$[10.13 \pm 0.240] \cdot 10^{-3}$ $([0.97, 10.61]10^{-3})$	F = 3.15 p = 0.056	SSD < HC (∗); p = 0.064; Cd = -0.58 SSD < AF (∗); p = 0.064; Cd = -0.57

Table S4. 2. Note: HC = Healthy Controls; SSD = Adolescent-Onset First-Episode Schizophrenia Spectrum Disorders; AF = Adolescent-Onset First-Episode Affective Psychosis patients; Q = Modularity; GE = Global Efficiency; LE = Local Efficiency; CO = Transition Cost; Di = Immobility; LS = Leap Size; CE = Cost Efficiency; μ = mean; CI = Confidence Intervals; SE = Standard Error; (∗∗) p<0.05; (∗) 0.09>p>0.05. Cd stands for Cohen's d.

Supplement 5. Graph measures

In this section, we include a detailed description of the graph measures analyzed in the main article. These include modularity, global and local efficiency, transition cost, immobility, and leap size.

- **Modularity (Q).** It measures the tendency of a graph to create clusters or modules[13], assuming that within a module the connection density between nodes is very large, whereas it decreases for nodes across different modules. In the current study, large modularity implies the recurrence of transitions to the same group of meta-states for relatively long periods, with eventual jumps to other groups of also highly-functionally-correlated meta-states. These modules (or communities) and their associated modularity were extracted using the Community Louvain algorithm[14].

- **Global and local efficiencies (GE and LE).** These are well-established metrics in network topology analysis[15] and represent how well-connected all different meta-states are. GE describes how efficiently a brain can transition from one meta-state to any other; whereas LE describes how efficiently the brain can transition from a specific meta-state to its closest neighbors. The average of local efficiencies was used for the current sample. The efficiency (E) is computed as follows:

$$E_{k^n} = \frac{1}{k^n(k^n-1)} \sum_{i \neq j \in k^n} \frac{1}{\delta_{ij}}$$

Where δ_{ij} represents the shortest path connecting meta-states *i* and *j* in the graph (for GE) or subgraph (for LE) considered.

- **Transition cost (CO).** This is a pondered measure of how many times the brain jumps between different meta-states. This depends on how dissimilar they are and may indirectly reflect the metabolic cost associated with such transitions.

$$CO_{k^n} = \left(J_{k^n} - R_{k^n}\right) \odot A_{k^n}$$

Where J_{k^n} is a $k^n \times k^n$ all-ones matrix and R_{k^n} is the correlation matrix between k^n meta-states.

- **Immobility (Im).** This measures the number of time-steps over the acquisition period during which the brain remains static, computed as the sum of the diagonal elements (or trace) of A_{k^n}.

$$Im_{k^n} = Trace\left(A_{k^n}\right)$$

- **Leap size (LS).** This is the ratio between the transition cost and the non-static behavior of the brain, which provides a normalized measure of metabolic cost[7].

$$LS_{k^n} = \frac{CO_{k^n}}{117 - median(D_{k^n})}$$

- **Cost-efficiency (CE).** This measures the balance between global efficiency and metabolic demands[16].

$$CE_{k^n} = \frac{GE_{k^n}}{CO_{k^n}}$$

References

1. Power JD, Schlaggar BL, Petersen SE. Recent progress and outstanding issues in motion correction in resting state fMRI. *Neuroimage*. 2015;105:536-551. doi:10.1016/j.neuroimage.2014.10.044

2. Parkes L, Fulcher B, Yücel M, Fornito A. An evaluation of the efficacy, reliability, and sensitivity of motion correction strategies for resting-state functional MRI. *Neuroimage*. 2018;171:415-436. doi:10.1016/j.neuroimage.2017.12.073

3. Pruim RHR, Mennes M, Buitelaar JK, Beckmann CF. Evaluation of ICA-AROMA and alternative strategies for motion artifact removal in resting state fMRI. *Neuroimage*. 2015;112:278-287. doi:10.1016/j.neuroimage.2015.02.063

4. Shine JM, Koyejo O, Bell PT, Gorgolewski KJ, Gilat M, Poldrack RA. Estimation of dynamic functional connectivity using Multiplication of Temporal Derivatives. *Neuroimage*. 2015;122:399-407. doi:10.1016/j.neuroimage.2015.07.064

5. O'Neill A, Carey E, Dooley N, et al. Multiple Network Dysconnectivity in Adolescents with Psychotic Experiences: A Longitudinal Population-Based Study. *Schizophr Bull*. 2020;46(6):1608-1618. doi:10.1093/schbul/sbaa056

6. Núñez P, Poza J, Gómez C, et al. Abnormal meta-state activation of dynamic brain networks across the Alzheimer spectrum. *Neuroimage*. 2021;232:117898. doi:10.1016/j.neuroimage.2021.117898

7. Ramirez-Mahaluf JP, Medel V, Tepper Á, et al. Transitions between human functional brain networks reveal complex, cost-efficient and behaviorally-relevant temporal paths. *Neuroimage*. 2020;219:117027. doi:10.1016/j.neuroimage.2020.117027

8. McInnes L, Healy J, Melville J. UMAP: Uniform Manifold Approximation and Projection for Dimension Reduction. 2018. http://arxiv.org/abs/1802.03426.

9. Rousseeuw PJ. Silhouettes: A graphical aid to the interpretation and validation of cluster analysis. *J Comput Appl Math*. 1987;20:53-65. doi:10.1016/0377-0427(87)90125-7

10. Du Y, Pearlson GD, Yu Q, et al. Interaction among subsystems within default mode network diminished in schizophrenia patients: A dynamic connectivity approach. *Schizophr Res*. 2016;170(1):55-65. doi:10.1016/j.schres.2015.11.021

11. Damaraju E, Allen EA, Belger A, et al. Dynamic functional connectivity analysis reveals transient states of dysconnectivity in schizophrenia. *NeuroImage Clin*. 2014;5:298-308. doi:10.1016/j.nicl.2014.07.003

12. Mair RW, Mcmains S. A Within-subject Comparison of Common Neuroimaging Protocols on MAGNETOM Prisma fit and MAGNETOM Trio Scanners. *MAGNETOM Flash*. 2017;(69):112-119.

13. Newman MEJ. Modularity and community structure in networks. *Proc Natl Acad Sci*. 2006;103(23):8577-8582. doi:10.1073/pnas.0601602103

14. Blondel VD, Guillaume J-L, Lambiotte R, Lefebvre E. Fast unfolding of communities in large networks. *J Stat Mech Theory Exp*. 2008;2008(10):P10008. doi:10.1088/1742-5468/2008/10/P10008

15. Latora V, Marchiori M. Efficient Behavior of Small-World Networks. *Phys Rev Lett*. 2001;87(19):198701. doi:10.1103/PhysRevLett.87.198701

16. Fornito A, Zalesky A, Bassett DS, et al. Genetic Influences on Cost-Efficient Organization of Human Cortical Functional Networks. *J Neurosci*. 2011;31(9):3261-3270. doi:10.1523/JNEUROSCI.4858-10.2011

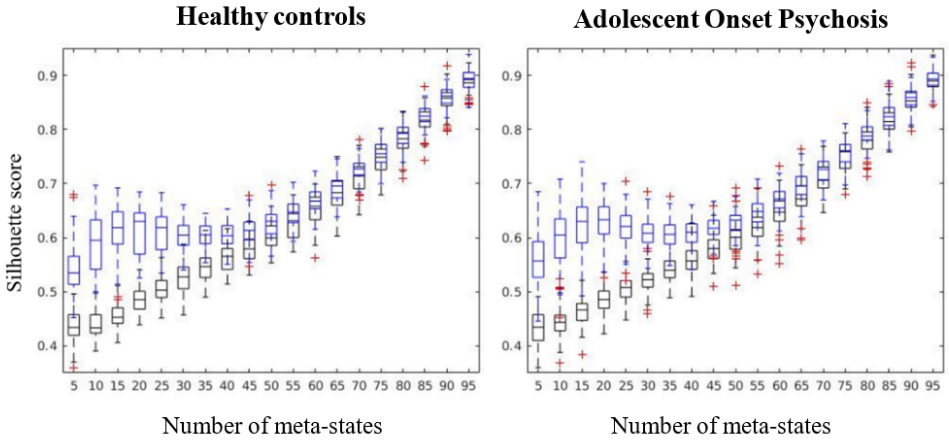

Distribution of Silhouette scores per kn clusters of connectivity matrices in a reduced space, both for healthy controls and first episode psychosis patients (blue), compared to that of null models (black).

556x261mm (47 x 47 DPI)

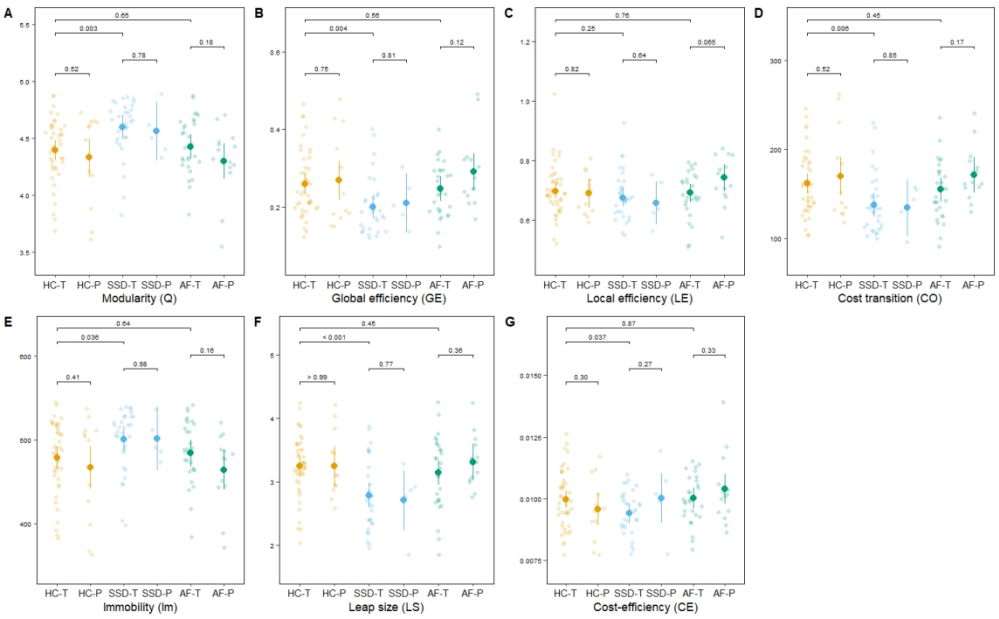

Estimated means and confidence intervals for the area under curve of each of the dynamic measures per group, in the subgroup of subjects scanned at the MAGNETOM Trio (T) scanner and its upgrade PrismaFit (P): HC (healthy controls, yellow), SSD (schizophrenia spectrum disorder AOP, blue), and AF (affective AOP, green). Uncorrected p-values for each group comparison are shown in each graph.

947x584mm (41 x 41 DPI)